

March 30, 2018



USGS California Fault Zone

LiDAR Technical Data Report

Contract No. G16PC00016, Task Order G17PD00970



Patrick Emmett
US Geological Survey
MS 666, 1400 Independence Road
Rolla, MO 65401
PH: 202-423-5089



QSI Corvallis
517 SW 2nd St., Suite 400
Corvallis, OR 97333
PH: 541-752-1204

TABLE OF CONTENTS

INTRODUCTION	5
Deliverable Products	6
ACQUISITION	8
Planning.....	8
Airborne LiDAR Survey	9
Ground Control.....	10
Monumentation	10
Ground Survey Points (GSPs).....	12
Land Cover Check Points	13
PROCESSING	15
LiDAR Data.....	15
Feature Extraction.....	17
Hydroflattening and Water’s Edge Breaklines.....	17
RESULTS & DISCUSSION.....	18
LiDAR Density	18
LiDAR Accuracy Assessments	22
LiDAR Non-Vegetated Vertical Accuracy	22
LiDAR Vegetated Vertical Accuracy	25
LiDAR Relative Vertical Accuracy	26
CERTIFICATIONS	27
SELECTED IMAGES.....	28
GLOSSARY	29
APPENDIX A - ACCURACY CONTROLS	30

Cover Photo: A view looking over a dry river bed in the Kelso Dunes Wilderness Area, created from the gridded bare earth model colored by elevation and intensity value.

INTRODUCTION

This photo taken by QSI acquisition staff shows a view desert and mixed shrubs in the USGS CA Fault Zone landscape in California.



In July 2017, Quantum Spatial (QSI) was contracted by the United States Geological Survey (USGS) as part of their 3DEP initiative, to collect Light Detection and Ranging (LiDAR) data in the summer of 2017 for the USGS California Fault Zone site in southern California (Task Order G17PD00970). Data were collected to aid USGS in assessing the topographic and geophysical properties of the study area to support the 3DEP mapping initiative and seismic hazard assessment of several sites within the project area.

This report accompanies the delivered LiDAR data and documents contract specifications, data acquisition procedures, processing methods, and analysis of the final dataset including LiDAR accuracy and density. Acquisition dates and acreage are shown in Table 1, a complete list of contracted deliverables provided to USGS is shown in Table 2, and the project extent is shown in Figure 1.

Table 1: Acquisition dates, acreage, and data types collected on the USGS California Fault Zone site

Project Site	Contracted Acres	Buffered Acres	Acquisition Dates	Data Type
USGS California Fault Zone	1,007,454	1,021,407	08/05/2017 – 08/22/2017	LiDAR

Deliverable Products

Table 2: Products delivered to USGS for the USGS California Fault Zone sites

California Fault Zone LiDAR Products Projection: UTM Zone 11 North Horizontal Datum: NAD83 (2011) Vertical Datum: NAVD88 (GEOID12B) Units: Meters	
Points	LAS v 1.4 <ul style="list-style-type: none"> • All Classified Returns • Flightline Swaths
Rasters	0.5 Meter ERDAS Imagine Files (*.img) <ul style="list-style-type: none"> • Hydroflattened Bare Earth Model (DEM) • Highest Hit Digital Surface Model (DSM) 0.5 Meter GeoTiffs <ul style="list-style-type: none"> • Intensity Images
Vectors	Shapefiles (*.shp) <ul style="list-style-type: none"> • Area of Interest • LiDAR Tile Index • DEM Tile Index • Water’s Edge Breaklines (with Z values) • Ground Survey Data • Flightline Index

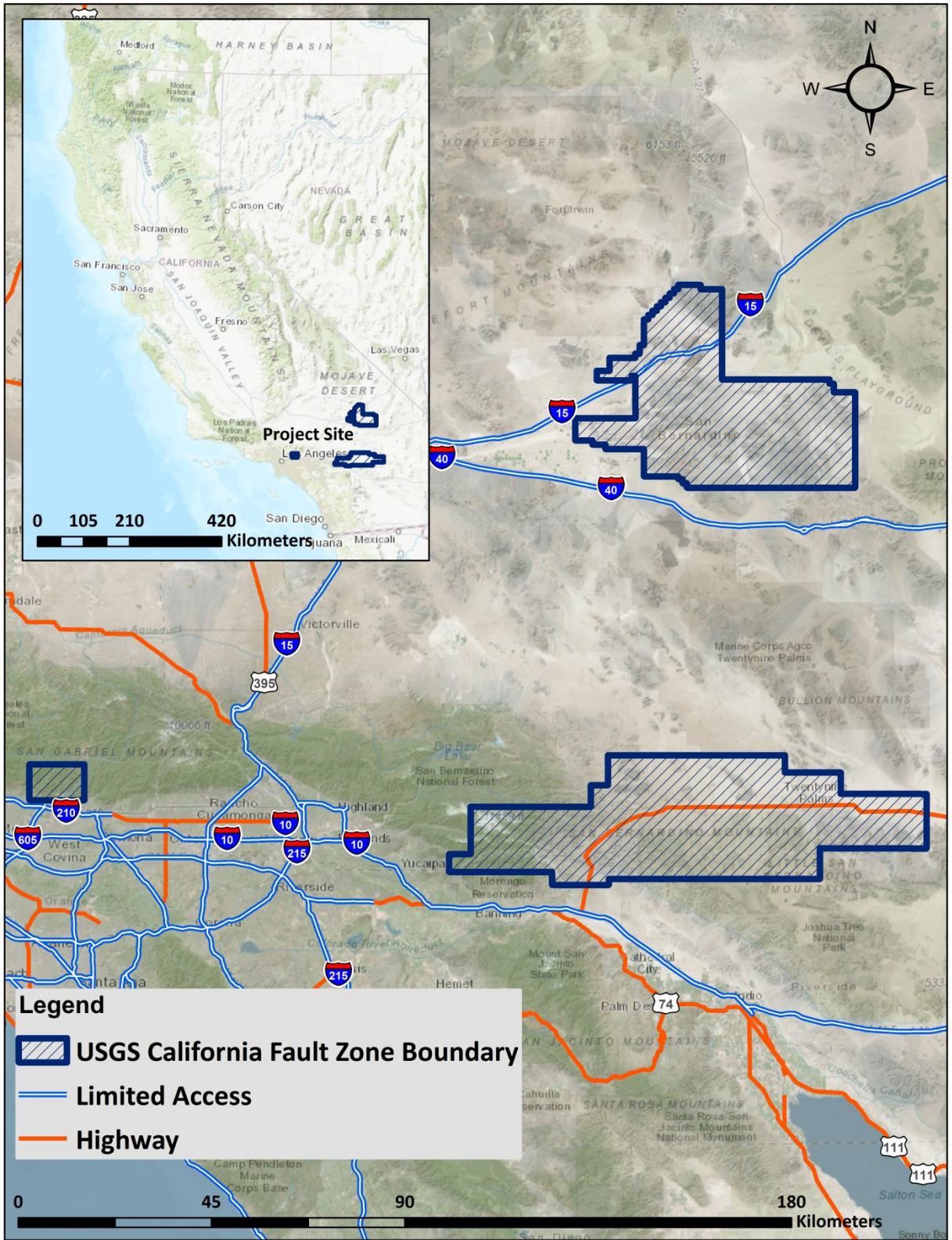


Figure 1: Location map of the USGS California Fault Zone site in California

This scenic photo taken by QSI's acquisition staff shows a view of the geologic features within the California Fault Zone project area.



Planning

In preparation for data collection, QSI reviewed the project area and developed a specialized flight plan to ensure complete coverage of the USGS California Fault Zone LiDAR study area at the target point density of ≥ 8.0 points/m². Acquisition parameters including orientation relative to terrain, flight altitude, pulse rate, scan angle, and ground speed were adapted to optimize flight paths and flight times while meeting all contract specifications.

Factors such as satellite constellation availability and weather windows must be considered during the planning stage. Any weather hazards or conditions affecting the flights were continuously monitored due to their potential impact on the daily success of airborne and ground operations. In addition, logistical considerations including private property access and potential air space restrictions were reviewed.

Airborne LiDAR Survey

The LiDAR survey was accomplished using a Leica ALS80 system mounted in a Cessna Caravan. Table 3 summarizes the settings used to yield an average pulse density of ≥ 8 pulses/m² over the USGS California Fault Zone project area. The Leica ALS80 laser system can record unlimited range measurements (returns) per pulse. It is not uncommon for some types of surfaces (e.g., dense vegetation or water) to return fewer pulses to the LiDAR sensor than the laser originally emitted. The discrepancy between first return and overall delivered density will vary depending on terrain, land cover, and the prevalence of water bodies. All discernible laser returns were processed for the output dataset.

Table 3: LiDAR specifications and survey settings

LiDAR Survey Settings & Specifications	
Acquisition Dates	August 5 – 22, 2017
Aircraft Used	Cessna Caravan
Sensor	Leica
Laser	ALS80
Maximum Returns	Unlimited
Resolution/Density	Average 8 pulses/m ²
Nominal Pulse Spacing	0.35 m
Survey Altitude (AGL)	1,650 m
Survey speed	140 knots
Field of View	30°
Mirror Scan Rate	48.0 Hz
Target Pulse Rate	330.4 kHz
Pulse Length	2.5 ns
Laser Pulse Footprint Diameter	36 cm
Central Wavelength	1064 nm
Pulse Mode	Single Pulse in Air (SPiA)
Beam Divergence	22 mrad
Swath Width	884 m
Swath Overlap	63%
Intensity	8-bit, scaled to 16-bit
Accuracy	RMSE _z (Non-Vegetated) ≤ 10 cm
	NVA (95% Confidence Level) ≤ 19.6 cm
	VVA (95 th Percentile) ≤ 29.4 cm



Leica ALS80 LiDAR sensor

All areas were surveyed with an opposing flightline side-lap of $\geq 50\%$ ($\geq 100\%$ overlap) in order to reduce laser shadowing and increase surface laser painting. To accurately solve for laser point position (geographic coordinates x, y, and z), the positional coordinates of the airborne sensor and the attitude of the aircraft were recorded continuously throughout the LiDAR data collection mission. Position of the aircraft was measured twice per second (2 Hz) by an onboard differential GPS unit, and aircraft attitude was measured 200 times per second (200 Hz) as pitch, roll, and yaw (heading) from an onboard inertial

measurement unit (IMU). To allow for post-processing correction and calibration, aircraft and sensor position and attitude data are indexed by GPS time.

Ground Control

Ground control surveys, including monumentation and ground survey points (GSPs), were conducted to support the airborne acquisition. Ground control data were used to geospatially correct the aircraft positional coordinate data and to perform quality assurance checks on final LiDAR data



Existing NGS Monument



QSI-Established Monument

Monumentation

The spatial configuration of ground survey monuments provided redundant control within 13 nautical miles of the mission areas for LiDAR flights. Monuments were also used for collection of ground survey points using real time kinematic (RTK), post processed kinematic (PPK), and fast static (FS) survey techniques.

Monument locations were selected with consideration for satellite visibility, field crew safety, and optimal location for GSP coverage. QSI utilized five existing monuments and established fourteen new monuments for the USGS California Fault Zone LiDAR project (Table 4, Figure 2). New monumentation was set using 5/8" x 30" rebar topped with stamped 2 ½ " aluminum caps. QSI's professional land surveyor, Evon P. Silvia (CAPLS#9401) oversaw and certified the establishment of all monuments.

Table 4: Monuments utilized/established for the USGS California Fault Zone acquisition. Coordinates are on the NAD83 (2011) datum, epoch 2010.00.

Monument ID	Latitude	Longitude	Ellipsoid (meters)
CALTRANS_BM_62	34° 02' 34.68274"	-116° 35' 04.46219"	758.370
CA_FAULTS_01	34° 10' 17.82822"	-116° 04' 16.83272"	541.762
CA_FAULTS_02	34° 02' 38.47470"	-116° 11' 55.23479"	1176.790
CA_FAULTS_03	34° 07' 13.91378"	-116° 20' 14.25582"	938.869
CA_FAULTS_04	34° 47' 19.33869"	-116° 27' 10.88438"	548.356
CA_FAULTS_05	34° 52' 46.90721"	-116° 34' 02.81490"	511.101
CA_FAULTS_06	35° 04' 17.34606"	-116° 24' 51.38843"	507.456
CA_FAULTS_07	35° 05' 18.01990"	-116° 20' 19.80190"	441.882
CA_FAULTS_08	34° 51' 20.95321"	-116° 12' 03.62313"	364.592
CA_FAULTS_09	34° 50' 08.59026"	-116° 12' 21.91899"	384.042
CA_FAULTS_10	34° 57' 35.14206"	-116° 08' 30.70195"	438.814
CA_FAULTS_12	33° 59' 55.27516"	-116° 36' 17.27906"	580.725

Monument ID	Latitude	Longitude	Ellipsoid (meters)
CA_FAULTS_13	33° 59' 56.59467"	-116° 54' 37.48065"	1197.780
CA_FAULTS_14	34° 49' 41.42131"	-115° 56' 48.03866"	634.832
EU0439	34° 08' 11.65178"	-115° 55' 52.75833"	505.055
EU0442	34° 08' 12.11917"	-115° 56' 57.17617"	530.976
EV9357	34° 09' 00.44090"	-117° 55' 50.39105"	175.851
G724_RESET	34° 08' 05.93331"	-116° 10' 39.81974"	720.300

To correct the continuously recorded onboard measurements of the aircraft position, QSI concurrently conducted multiple static Global Navigation Satellite System (GNSS) ground surveys (1 Hz recording frequency) over each monument. During post-processing, the static GPS data were triangulated with nearby Continuously Operating Reference Stations (CORS) using the Online Positioning User Service (OPUS¹) for precise positioning. Multiple independent sessions over the same monument were processed to confirm antenna height measurements and to refine position accuracy.

Monuments were established according to the national standard for geodetic control networks, as specified in the Federal Geographic Data Committee (FGDC) Geospatial Positioning Accuracy Standards for geodetic networks.² This standard provides guidelines for classification of monument quality at the 95% confidence interval as a basis for comparing the quality of one control network to another. The monument rating for this project is shown in Table 5.

Table 5: Federal Geographic Data Committee monument rating for network accuracy

Direction	Rating
1.96 * St Dev _{NE} :	0.050 m
1.96 * St Dev _Z :	0.050 m

For the USGS California Fault Zone LiDAR project, the monument coordinates contributed no more than 5.4 cm of positional error to the geolocation of the final ground survey points and LiDAR, with 95% confidence.

¹ OPUS is a free service provided by the National Geodetic Survey to process corrected monument positions. <http://www.ngs.noaa.gov/OPUS>.

² Federal Geographic Data Committee, Geospatial Positioning Accuracy Standards (FGDC-STD-007.2-1998). Part 2: Standards for Geodetic Networks, Table 2.1, page 2-3. <http://www.fgdc.gov/standards/projects/FGDC-standards-projects/accuracy/part2/chapter2>

Ground Survey Points (GSPs)

Ground survey points were collected using real time kinematic (RTK) and fast-static (FS) survey techniques. A Trimble R7 base unit was positioned at a nearby monument to broadcast a kinematic correction to a roving Trimble R8 GNSS receiver. All GSP measurements were made during periods with a Position Dilution of Precision (PDOP) of ≤ 3.0 with at least six satellites in view of the stationary and roving receivers. When collecting RTK and PPK data, the rover records data while stationary for five seconds, then calculates the pseudorange position using at least three one-second epochs. FS surveys record observations for up to fifteen minutes on each GSP in order to support longer baselines for post-processing. Relative errors for any GSP position must be less than 1.5 cm horizontal and 2.0 cm vertical in order to be accepted. See Table 6 for Trimble unit specifications.

GSPs were collected in areas where good satellite visibility was achieved on paved roads and other hard surfaces such as gravel or packed dirt roads. GSP measurements were not taken on highly reflective surfaces such as center line stripes or lane markings on roads due to the increased noise seen in the laser returns over these surfaces. GSPs were collected within as many flightlines as possible; however the distribution of GSPs depended on ground access constraints and monument locations and may not be equitably distributed throughout the study area (Figure 2).





Table 6: Trimble equipment identification

Receiver Model	Antenna	OPUS Antenna ID	Use
Trimble R7 GNSS	Zephyr GNSS Geodetic Model 2 RoHS	TRM57971.00	Static
Trimble R8	Integrated Antenna R8 Model 2	TRM_R8_GNSS	Static, Rover

Land Cover Check Points

In addition to ground survey points, check points were collected throughout the study area, using land class descriptions, to evaluate vegetated and non-vegetated vertical accuracy. Vertical accuracy statistics were calculated for all land cover types to assess confidence in the LiDAR derived ground models across land cover classes (Table 7, see LiDAR Accuracy Assessments, page 22).

Table 7: Land Cover Types and Descriptions

Land cover type	Land cover code	Example	Description	Accuracy Assessment Type
Shrub	SHRUB		Areas dominated by herbaceous shrubland	VVA
Forest	FOREST		Areas of mixed forested growth	VVA
Bare Earth	BARE		Areas of bare earth surface	NVA
Urban	URBAN		Areas dominated by urban development, including parks	NVA

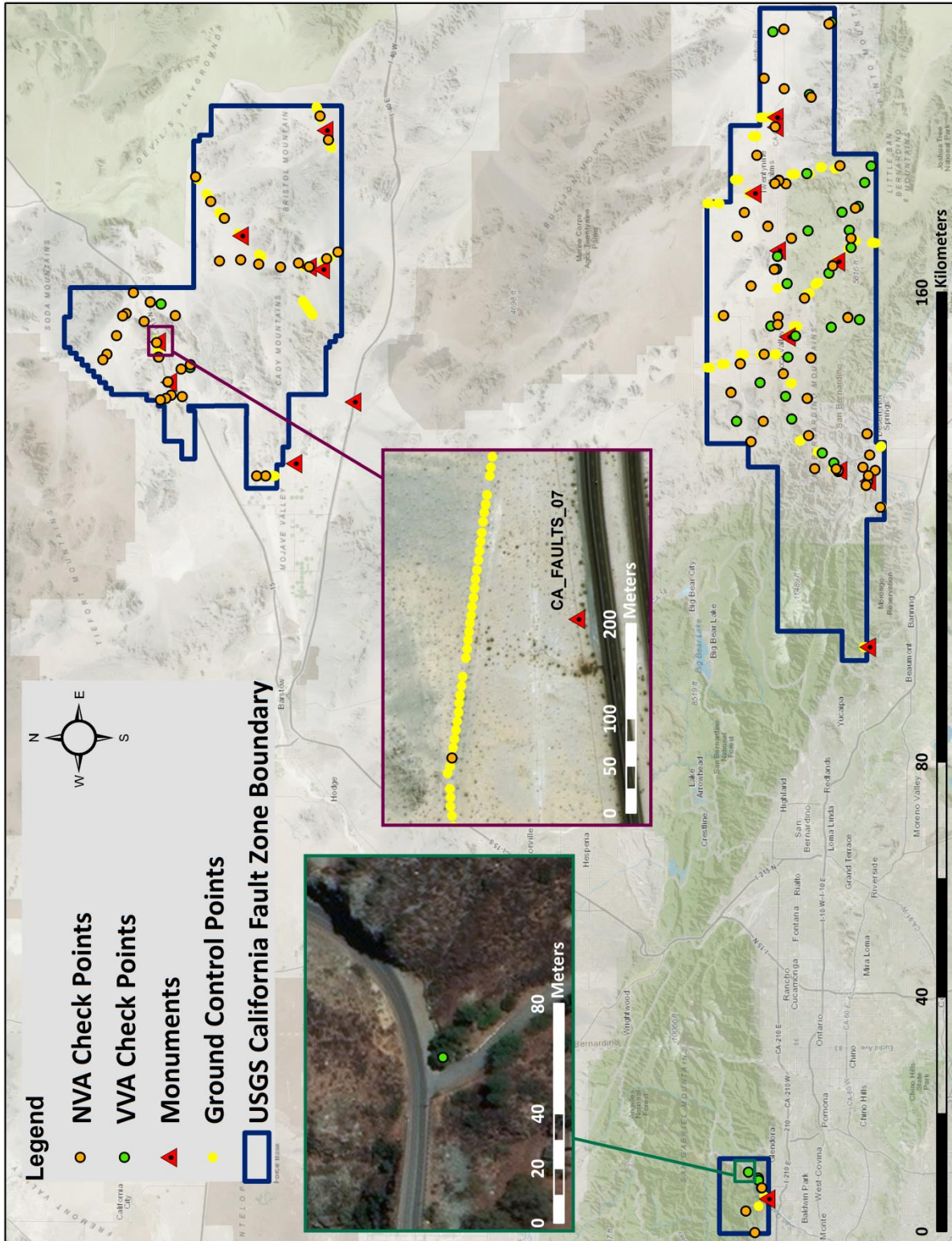
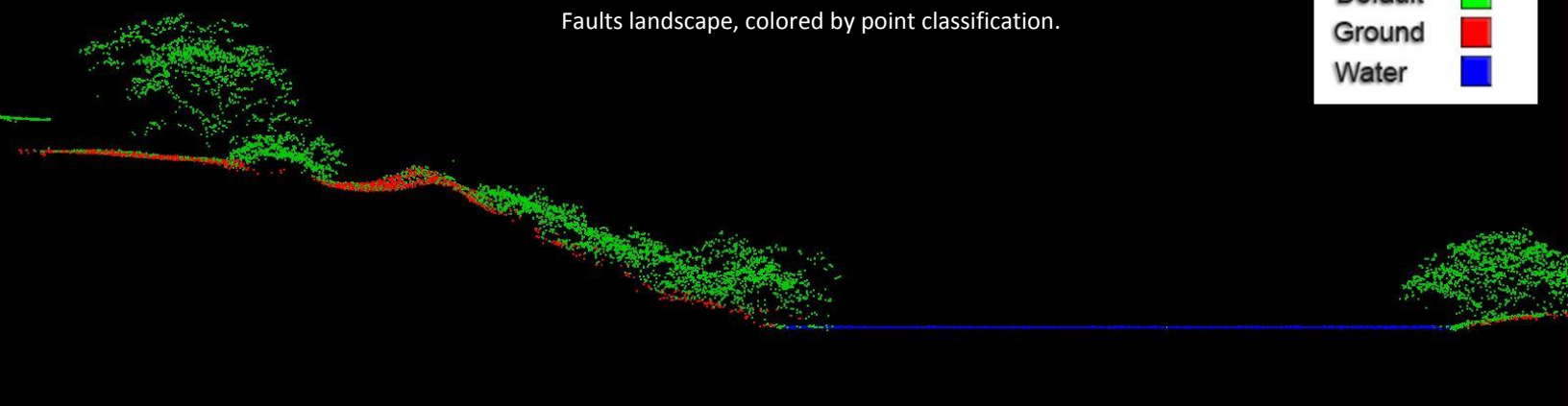


Figure 2: Ground survey location map

PROCESSING

This LiDAR cross section shows a view of the California Faults landscape, colored by point classification.



LiDAR Data

Upon completion of data acquisition, QSI processing staff initiated a suite of automated and manual techniques to process the data into the requested deliverables. Processing tasks included GPS control computations, smoothed best estimate trajectory (SBET) calculations, kinematic corrections, calculation of laser point position, sensor and data calibration for optimal relative and absolute accuracy, and LiDAR point classification (Table 8). Processing methodologies were tailored for the landscape. Brief descriptions of these tasks are shown in Table 9.

Table 8: ASPRS LAS classification standards applied to the USGS California Fault Zone dataset

Classification Number	Classification Name	Classification Description
1	Default/Unclassified	Laser returns that are not included in the ground class, composed of vegetation and anthropogenic features
10	Overlap	Flightline edge clip return that are flagged with overlap and withheld flags.
2	Ground	Laser returns that are determined to be ground using automated and manual cleaning algorithms
7	Noise	Laser returns that are often associated with birds, scattering from reflective surfaces, or artificial points below the ground surface
9	Water	Laser returns that are determined to be water using automated and manual cleaning algorithms
10	Ignored Ground	Ground points proximate to water's edge breaklines; ignored for correct model creation
17	Bridge	Bridge decks

Table 9: LiDAR processing workflow

LiDAR Processing Step	Software Used
Resolve kinematic corrections for aircraft position data using kinematic aircraft GPS and static ground GPS data. Develop a smoothed best estimate of trajectory (SBET) file that blends post-processed aircraft position with sensor head position and attitude recorded throughout the survey.	Waypoint Inertial Explorer v.8.6
Calculate laser point position by associating SBET position to each laser point return time, scan angle, intensity, etc. Create raw laser point cloud data for the entire survey in *.las (ASPRS v. 1.2) format. Convert data to orthometric elevations by applying a geoid correction.	Waypoint Inertial Explorer v.8.6 Leica Cloudpro v. 1.2.2
Import raw laser points into manageable blocks (less than 500 MB) to perform manual relative accuracy calibration and filter erroneous points. Classify ground points for individual flightlines.	TerraScan v.17
Using ground classified points per each flightline, test the relative accuracy. Perform automated line-to-line calibrations for system attitude parameters (pitch, roll, heading), mirror flex (scale) and GPS/IMU drift. Calculate calibrations on ground classified points from paired flightlines and apply results to all points in a flightline. Use every flightline for relative accuracy calibration.	TerraMatch v.17
Classify resulting data to ground and other client designated ASPRS classifications (Table 8). Assess statistical absolute accuracy via direct comparisons of ground classified points to ground control survey data.	TerraScan v.17 TerraModeler v.17
Generate bare earth models as triangulated surfaces. Generate highest hit models as a surface expression of all classified points. Export all surface models in EDRAS Imagine (.img) format at a 0.5 meter pixel resolution.	TerraScan v.17 TerraModeler v.17 ArcMap v. 10.2.2
Export intensity images as GeoTIFFs at a 0.5 meter pixel resolution.	Las Monkey 2.2.8 (QSI proprietary) LAS Product Creator 1.5 (QSI proprietary) ArcMap v. 10.2.2

Feature Extraction

Hydroflattening and Water's Edge Breaklines

Water bodies within the USGS California Fault Zone project area were flattened to a consistent water level. Bodies of water that were flattened include lakes and other closed water bodies with a surface area greater than 2 acres, and select smaller bodies of water as feasible. The hydroflattening process eliminates artifacts in the digital terrain model caused by both increased variability in ranges or dropouts in laser returns due to the low reflectivity of water.

Hydroflattening of closed water bodies was performed through a combination of automated and manual detection and adjustment techniques designed to identify water boundaries and water levels. Boundary polygons were developed using an algorithm which weights LiDAR-derived slopes, intensities, and return densities to detect the water's edge. The water edges were then manually reviewed and edited as necessary.

Once polygons were developed the initial ground classified points falling within water polygons were reclassified as water points to omit them from the final ground model. Elevations were then obtained from the filtered LiDAR returns to create the final breaklines. Lakes were assigned a consistent elevation for an entire polygon.

Water boundary breaklines were then incorporated into the hydroflattened DEM by enforcing triangle edges (adjacent to the breakline) to the elevation values of the breakline. This implementation corrected interpolation along the hard edge. Water surfaces were obtained from a TIN of the 3D water edge breaklines resulting in the final hydroflattened model.

The same LiDAR cross section as above shows the California Faults landscape colored by point laser echo.



LiDAR Density

The acquisition parameters were designed to acquire an average first-return density of 8 points/m². First return density describes the density of pulses emitted from the laser that return at least one echo to the system. Multiple returns from a single pulse were not considered in first return density analysis. Some types of surfaces (e.g., breaks in terrain, water and steep slopes) may have returned fewer pulses than originally emitted by the laser. First returns typically reflect off the highest feature on the landscape within the footprint of the pulse. In forested or urban areas the highest feature could be a tree, building or power line, while in areas of unobstructed ground, the first return will be the only echo and represents the bare earth surface.

The density of ground-classified LiDAR returns was also analyzed for this project. Terrain character, land cover, and ground surface reflectivity all influenced the density of ground surface returns. In vegetated areas, fewer pulses may penetrate the canopy, resulting in lower ground density.

The average first-return density of LiDAR data for the USGS California Fault Zone project was 13.37 points/m² while the average ground classified density was 3.67 points/m² (Table 10). The statistical and spatial distributions of first return densities and classified ground return densities per 100 m x 100 m cell are portrayed in Figure 3 through Figure 6.

Table 10: Average LiDAR point densities

Classification	Point Density
First-Return	13.37 points/m ²
Ground Classified	3.67 points/m ²

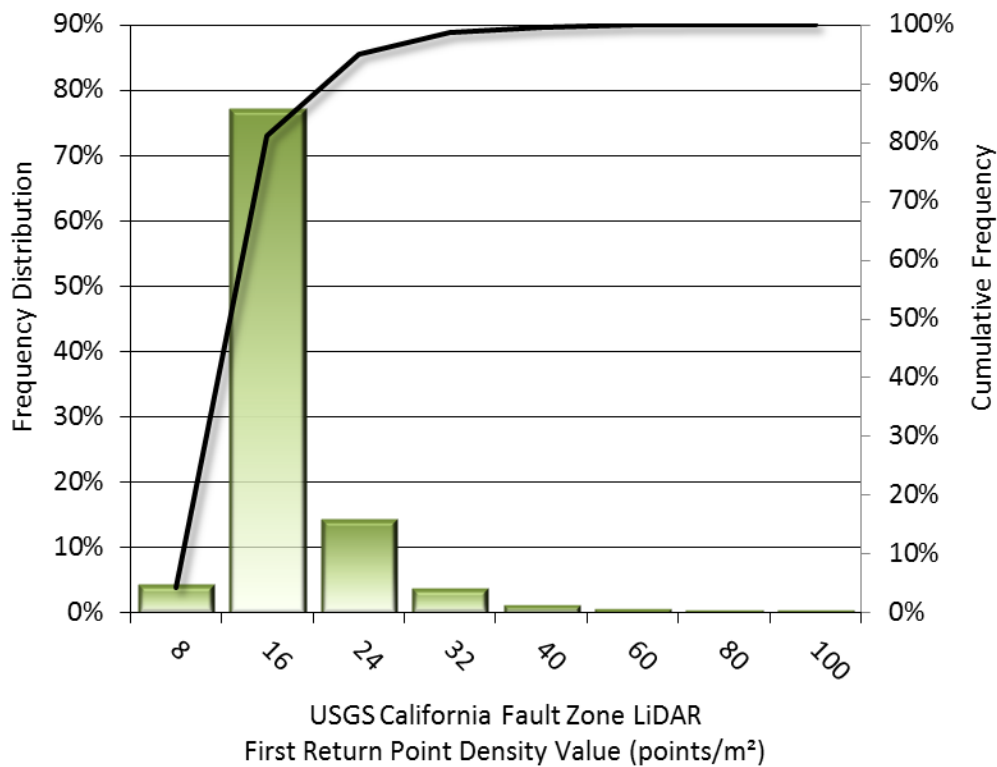


Figure 3: Frequency distribution of first return point density values per 100 x 100 m cell

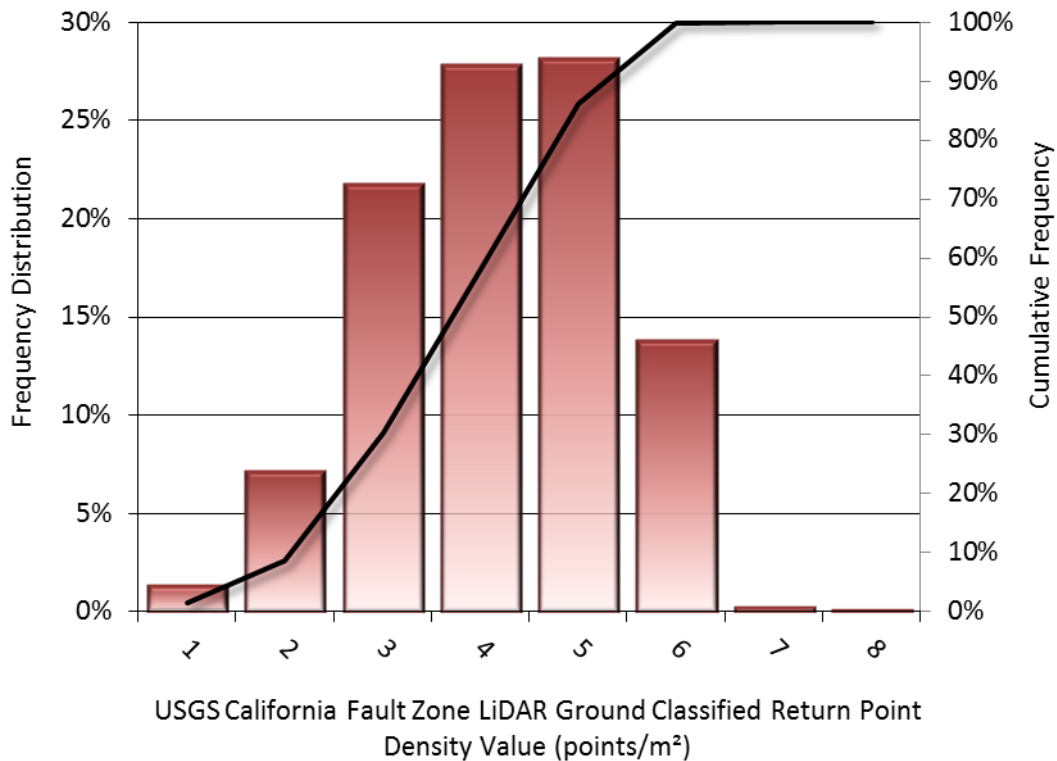


Figure 4: Frequency distribution of ground-classified return point density values per 100 x 100 m cell

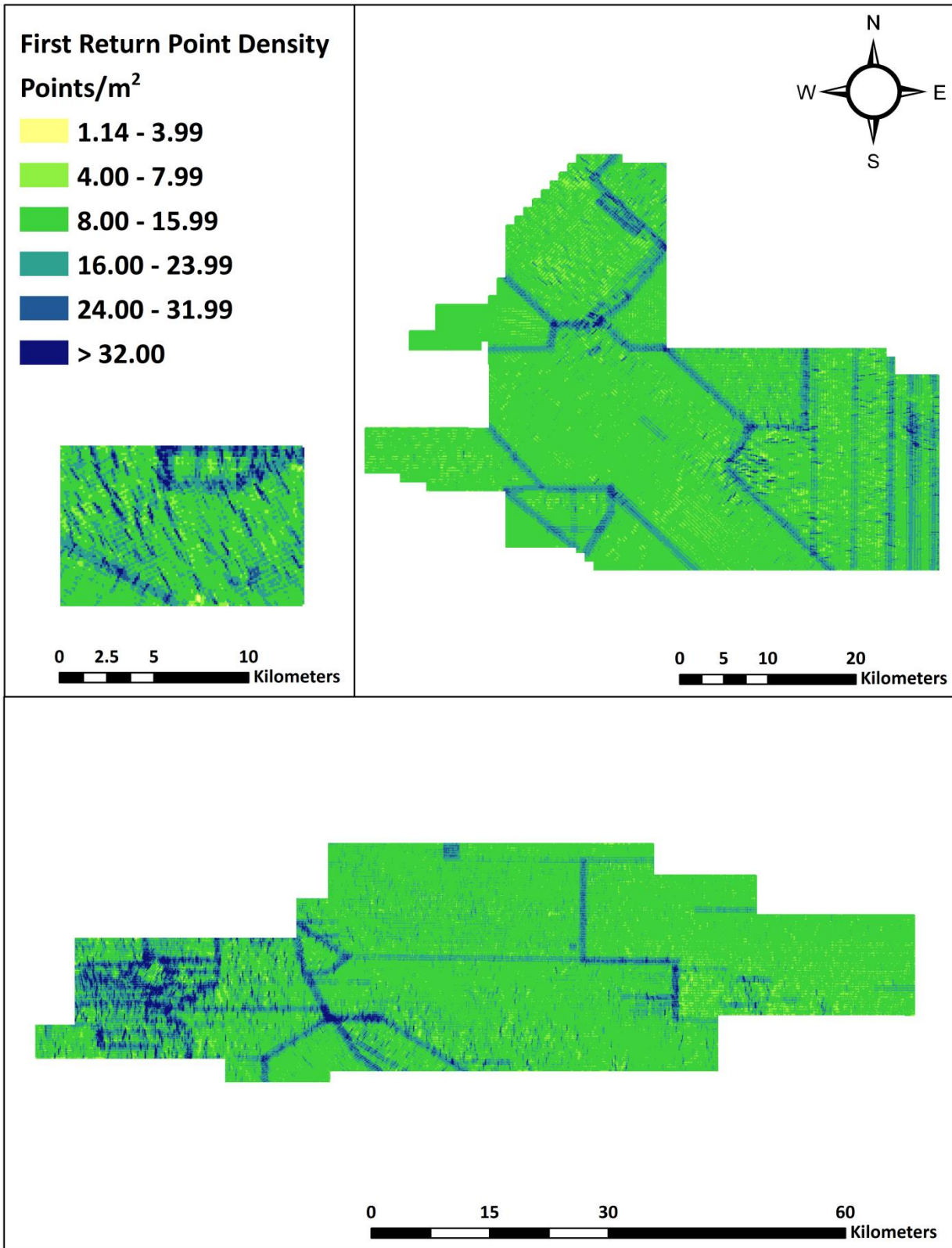


Figure 5: First return point density map for the USGS California Fault Zone site (100 m x 100 m cells)

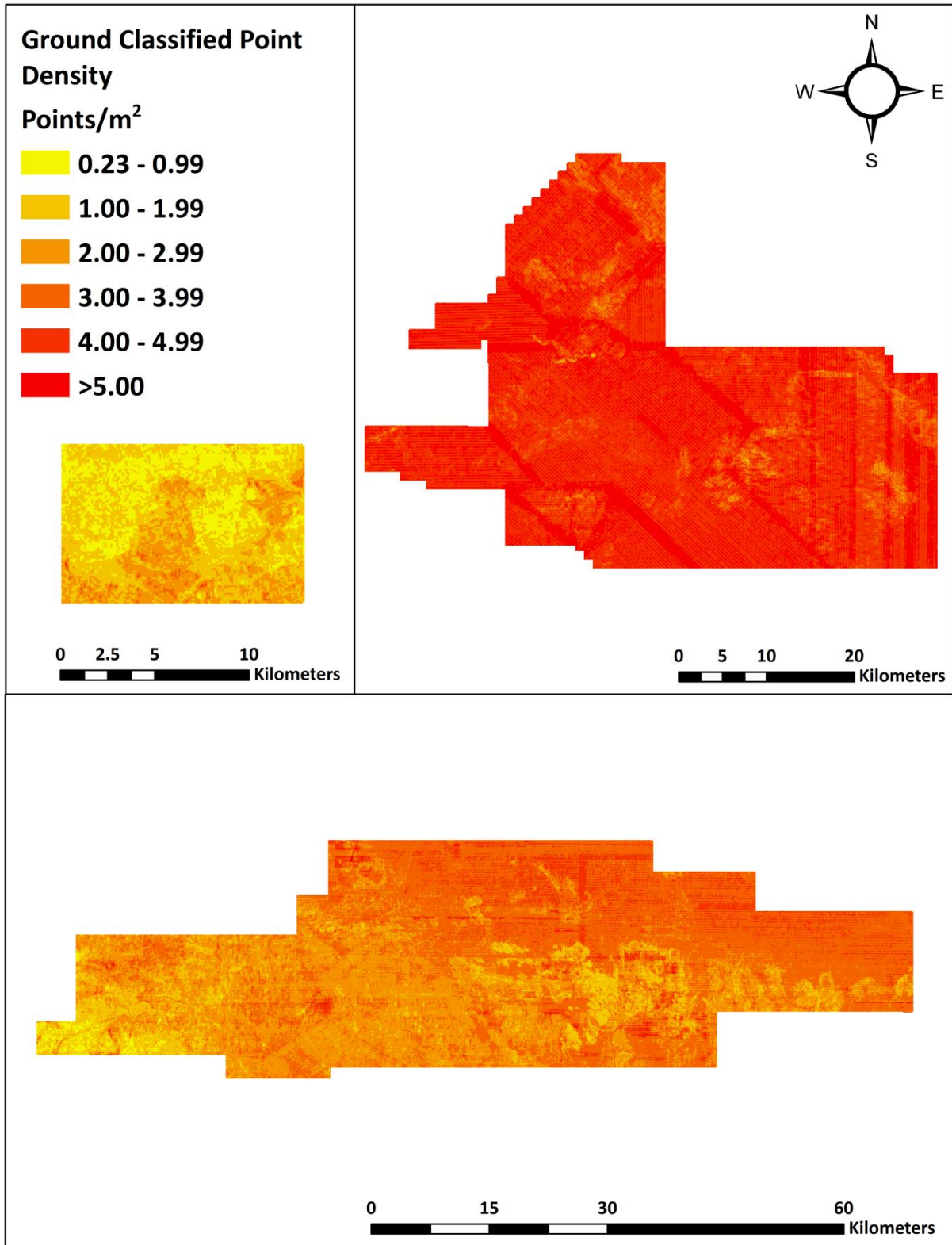


Figure 6: Ground classified point density map for the USGS California Fault Zone site (100 m x 100 m cells)

LiDAR Accuracy Assessments

The accuracy of the LiDAR data collection can be described in terms of absolute accuracy (the consistency of the data with external data sources) and relative accuracy (the consistency of the dataset with itself). See Appendix A for further information on sources of error and operational measures used to improve relative accuracy.

LiDAR Non-Vegetated Vertical Accuracy

Absolute accuracy was assessed using Non-Vegetated Vertical Accuracy (NVA) reporting designed to meet guidelines presented in the FGDC National Standard for Spatial Data Accuracy³. NVA compares known ground quality assurance point data collected on open, bare earth surfaces with level slope (<20°) to the triangulated surface generated by the LiDAR points. NVA is a measure of the accuracy of LiDAR point data in open areas where the LiDAR system has a high probability of measuring the ground surface and is evaluated at the 95% confidence interval (1.96 * RMSE), as shown in Table 11.

The mean and standard deviation (sigma σ) of divergence of the ground surface model from quality assurance point coordinates are also considered during accuracy assessment. These statistics assume the error for x, y and z is normally distributed, and therefore the skew and kurtosis of distributions are also considered when evaluating error statistics. For the USGS California Fault Zone survey, 96 quality assurance points were collected within the project area resulting in a non-vegetated vertical accuracy of 0.113 meters as compared to the bare earth DEM, and 0.102 meters as compared to the unclassified point cloud, with 95% confidence (Table 11, Figure 7, and Figure 8).

QSI also assessed absolute accuracy using 4,816 ground control points. Although these points were used in the calibration and post-processing of the LiDAR point cloud, they still provide a good indication of the overall accuracy of the LiDAR dataset, and therefore have been provided in Table 11 and Figure 9.

Table 11: Absolute accuracy results

Absolute Vertical Accuracy			
	NVA as compared to Bare Earth DEM	NVA as compared to unclassified LAS	Ground Control Points
Sample	80 points	80 points	4,816 points
95% Confidence (1.96*RMSE)	0.113 m	0.102 m	0.072 m
Average	-0.031 m	-0.016 m	0.001 m
Median	-0.022 m	-0.005 m	0.007 m
RMSE	0.058 m	0.052 m	0.037 m
Standard Deviation (1σ)	0.049 m	0.050 m	0.037 m

³ Federal Geographic Data Committee, ASPRS POSITIONAL ACCURACY STANDARDS FOR DIGITAL GEOSPATIAL DATA EDITION 1, Version 1.0, NOVEMBER 2014. <http://www.asprs.org/PAD-Division/ASPRS-POSITIONAL-ACCURACY-STANDARDS-FOR-DIGITAL-GEOSPATIAL-DATA.html>.

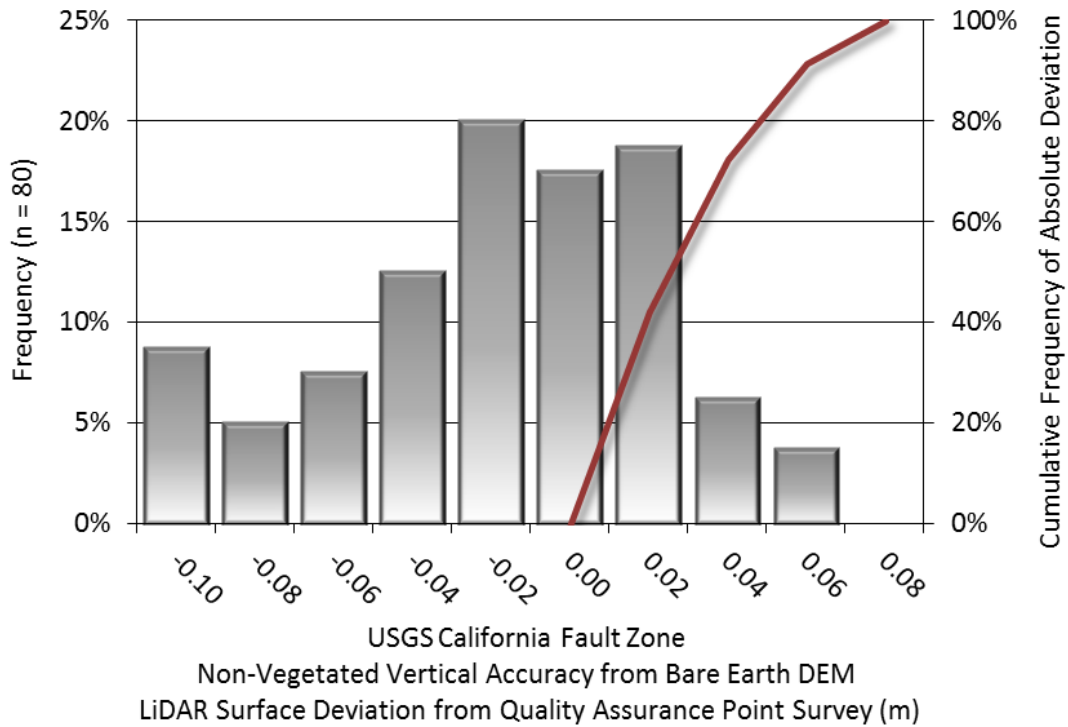


Figure 7: Frequency histogram for LiDAR bare earth surface deviation from quality assurance point values (NVA)

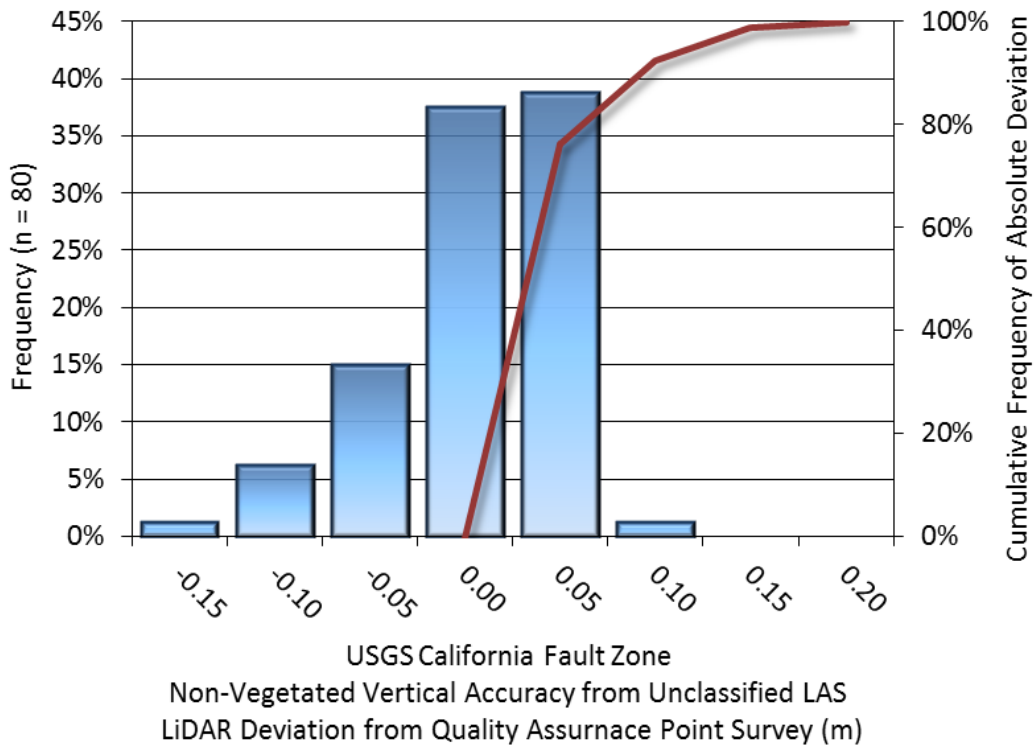


Figure 8: Frequency histogram for LiDAR unclassified LAS deviation from quality assurance point values (NVA)

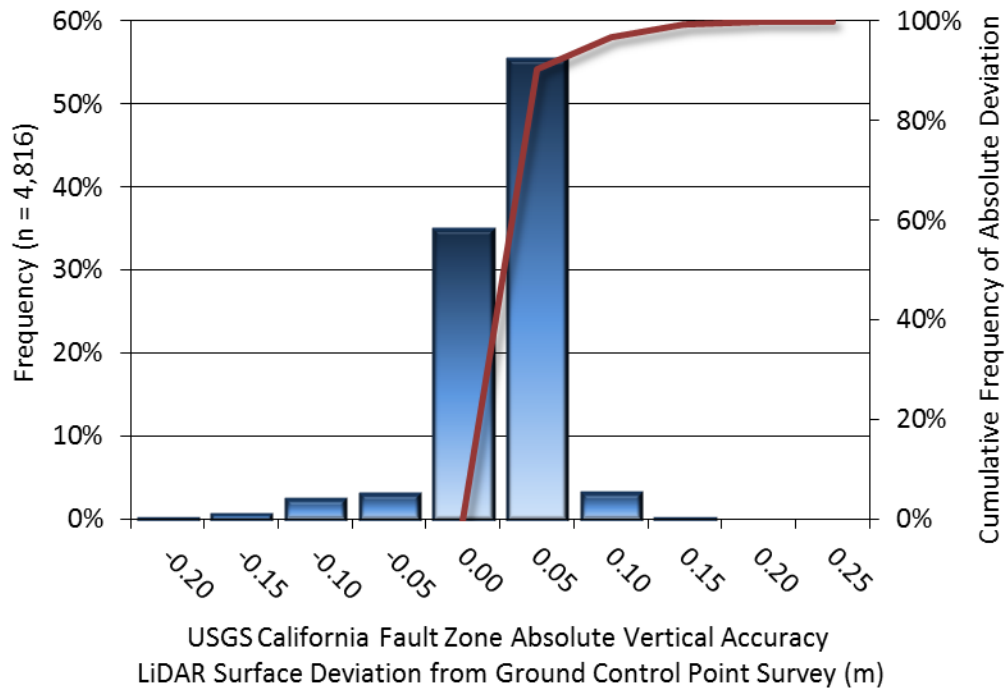


Figure 9: Frequency histogram for LiDAR surface deviation from ground control point values

LiDAR Vegetated Vertical Accuracy

QSI also assessed vertical accuracy using Vegetated Vertical Accuracy (VVA) reporting. VVA compares known ground check point data collected over vegetated surfaces using land class descriptions to the triangulated ground surface generated by the ground classified LiDAR points. For the USGS California Fault Zone survey, 61 vegetated check points were collected within the project area resulting in a vegetated vertical accuracy of 0.127 meters, evaluated at the 95th percentile (Table 11, Figure 8).

Table 12: Vegetated Vertical Accuracy Results

Vegetated Vertical Accuracy	
Sample	61 points
95 th Percentile	0.127 m
Average	-0.005 m
Median	-0.009 m
RMSE	0.066 m
Standard Deviation (1 σ)	0.066 m

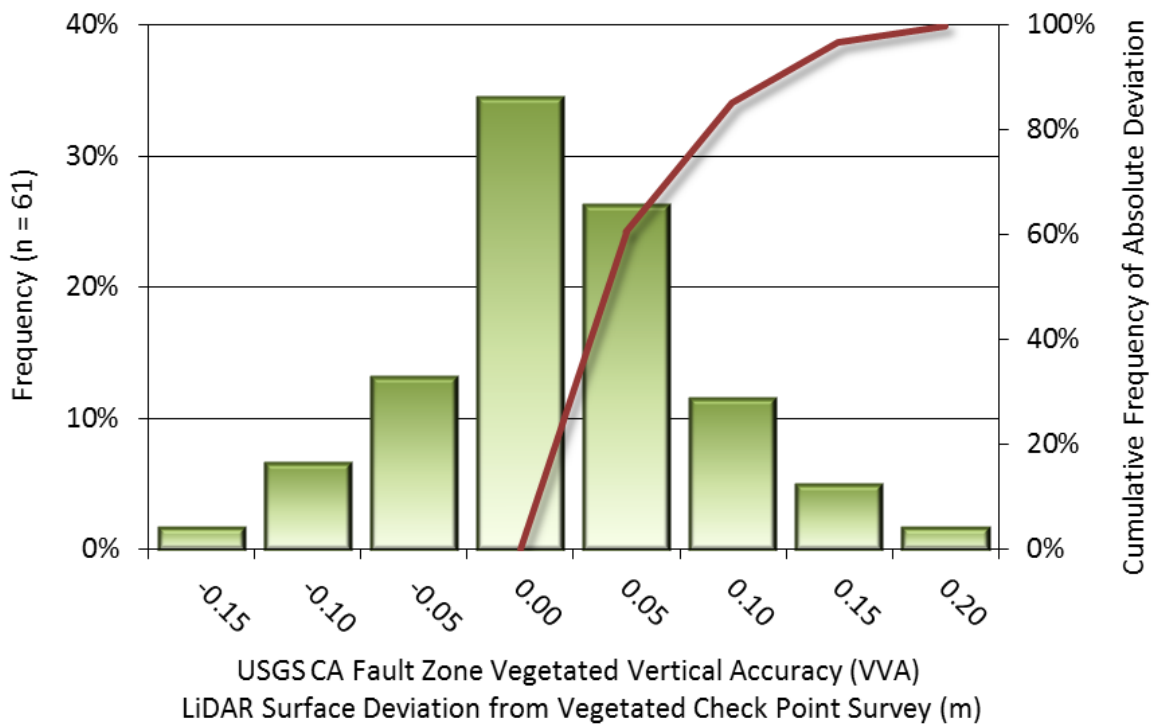


Figure 10: Frequency histogram for LiDAR surface deviation from vegetated check point values

LiDAR Relative Vertical Accuracy

Relative vertical accuracy refers to the internal consistency of the data set as a whole: the ability to place an object in the same location given multiple flightlines, GPS conditions, and aircraft attitudes. When the LiDAR system is well calibrated, the swath-to-swath vertical divergence is low (<0.10 meters). The relative vertical accuracy was computed by comparing the ground surface model of each individual flightline with its neighbors in overlapping regions. The average (mean) line to line relative vertical accuracy for the USGS California Fault Zone LiDAR project was 0.033 meters (Table 13, Figure 11).

Table 13: Relative accuracy results

Relative Accuracy	
Sample	971 surfaces
Average	0.033 m
Median	0.034 m
RMSE	0.043 m
Standard Deviation (1σ)	0.018 m
1.96 σ	0.035 m

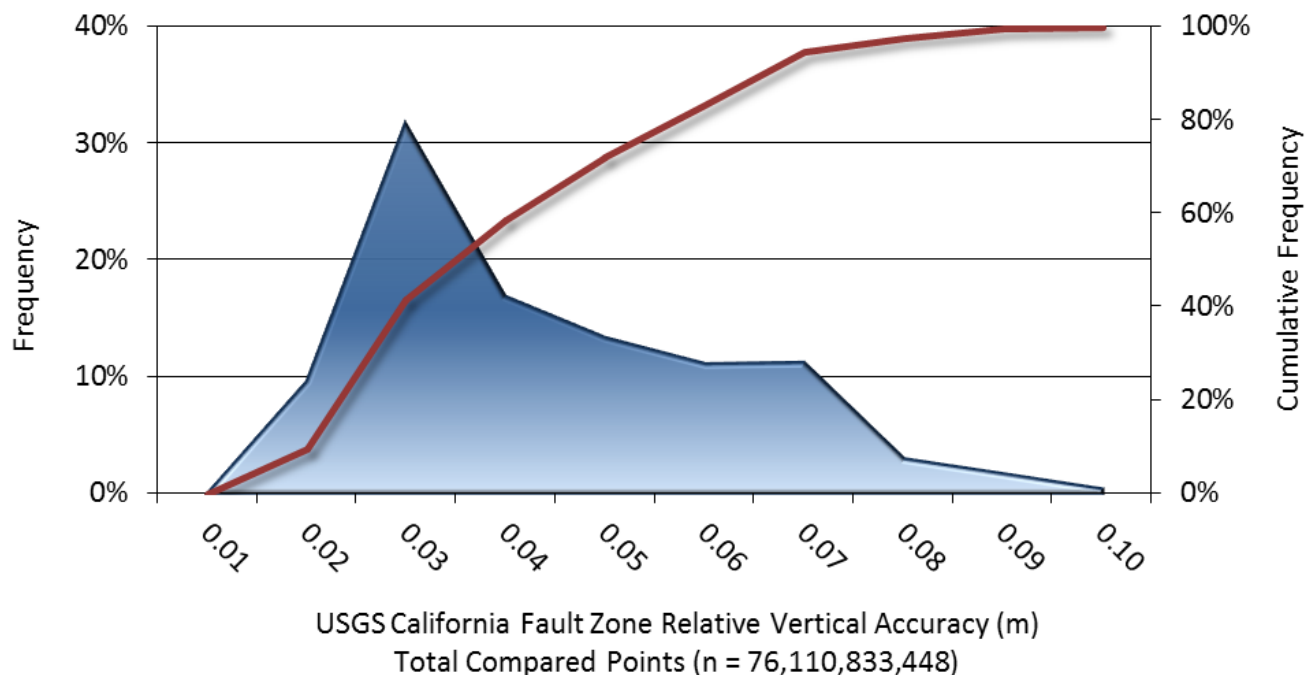
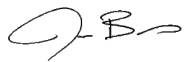


Figure 11: Frequency plot for relative vertical accuracy between flightlines

CERTIFICATIONS

Quantum Spatial, Inc. provided LiDAR services for the USGS California Fault Zone project as described in this report.

I, Joel Burroughs, have reviewed the attached report for completeness and hereby state that it is a complete and accurate report of this project.



Mar 30, 2018

Joel Burroughs
Project Manager
Quantum Spatial, Inc.

I, Evon P. Silvia, PLS, being duly registered as a Professional Land Surveyor in and by the state of California, hereby certify that the methodologies, static GNSS occupations used during airborne flights, and ground survey point collection were performed using commonly accepted Standard Practices. Field work conducted for this report was conducted between July 31 and August 22, 2017.

Accuracy statistics shown in the Accuracy Section of this Report have been reviewed by me and found to meet the "National Standard for Spatial Data Accuracy".



Mar 30, 2018

Evon P. Silvia, PLS
Quantum Spatial, Inc.
Corvallis, OR 97333



Signed: Mar 30, 2018

SELECTED IMAGES



Figure 12: View of the Kelso Wilderness Area in the California Fault Zone AOI. The image was created from the LiDAR bare earth model colored by elevation and intensity value.

1-sigma (σ) Absolute Deviation: Value for which the data are within one standard deviation (approximately 68th percentile) of a normally distributed data set.

1.96 * RMSE Absolute Deviation: Value for which the data are within two standard deviations (approximately 95th percentile) of a normally distributed data set, based on the FGDC standards for Non-vegetated Vertical Accuracy (NVA) reporting.

Accuracy: The statistical comparison between known (surveyed) points and laser points. Typically measured as the standard deviation (σ) and root mean square error (RMSE).

Absolute Accuracy: The vertical accuracy of LiDAR data is described as the mean and standard deviation (σ) of divergence of LiDAR point coordinates from ground survey point coordinates. To provide a sense of the model predictive power of the dataset, the root mean square error (RMSE) for vertical accuracy is also provided. These statistics assume the error distributions for x, y and z are normally distributed, and thus we also consider the skew and kurtosis of distributions when evaluating error statistics.

Relative Accuracy: Relative accuracy refers to the internal consistency of the data set; i.e., the ability to place a laser point in the same location over multiple flightlines, GPS conditions and aircraft attitudes. Affected by system attitude offsets, scale and GPS/IMU drift, internal consistency is measured as the divergence between points from different flightlines within an overlapping area. Divergence is most apparent when flightlines are opposing. When the LiDAR system is well calibrated, the line-to-line divergence is low (<10 cm).

Root Mean Square Error (RMSE): A statistic used to approximate the difference between real-world points and the LiDAR points. It is calculated by squaring all the values, then taking the average of the squares and taking the square root of the average.

Data Density: A common measure of LiDAR resolution, measured as points per square meter.

Digital Elevation Model (DEM): File or database made from surveyed points, containing elevation points over a contiguous area. Digital terrain models (DTM) and digital surface models (DSM) are types of DEMs. DTMs consist solely of the bare earth surface (ground points), while DSMs include information about all surfaces, including vegetation and man-made structures.

Intensity Values: The peak power ratio of the laser return to the emitted laser, calculated as a function of surface reflectivity.

Nadir: A single point or locus of points on the surface of the earth directly below a sensor as it progresses along its flightline.

Overlap: The area shared between flightlines, typically measured in percent. 100% overlap is essential to ensure complete coverage and reduce laser shadows.

Pulse Rate (PR): The rate at which laser pulses are emitted from the sensor; typically measured in thousands of pulses per second (kHz).

Pulse Returns: For every laser pulse emitted, the number of wave forms (i.e., echoes) reflected back to the sensor. Portions of the wave form that return first are the highest element in multi-tiered surfaces such as vegetation. Portions of the wave form that return last are the lowest element in multi-tiered surfaces.

Real-Time Kinematic (RTK) Survey: A type of surveying conducted with a GPS base station deployed over a known monument with a radio connection to a GPS rover. Both the base station and rover receive differential GPS data and the baseline correction is solved between the two. This type of ground survey is accurate to 1.5 cm or less.

Post-Processed Kinematic (PPK) Survey: GPS surveying is conducted with a GPS rover collecting concurrently with a GPS base station set up over a known monument. Differential corrections and precisions for the GNSS baselines are computed and applied after the fact during processing. This type of ground survey is accurate to 1.5 cm or less.

Scan Angle: The angle from nadir to the edge of the scan, measured in degrees. Laser point accuracy typically decreases as scan angles increase.

Native LiDAR Density: The number of pulses emitted by the LiDAR system, commonly expressed as pulses per square meter.

APPENDIX A - ACCURACY CONTROLS

Relative Accuracy Calibration Methodology:

Manual System Calibration: Calibration procedures for each mission require solving geometric relationships that relate measured swath-to-swath deviations to misalignments of system attitude parameters. Corrected scale, pitch, roll and heading offsets were calculated and applied to resolve misalignments. The raw divergence between lines was computed after the manual calibration was completed and reported for each survey area.

Automated Attitude Calibration: All data were tested and calibrated using TerraMatch automated sampling routines. Ground points were classified for each individual flightline and used for line-to-line testing. System misalignment offsets (pitch, roll and heading) and scale were solved for each individual mission and applied to respective mission datasets. The data from each mission were then blended when imported together to form the entire area of interest.

Automated Z Calibration: Ground points per line were used to calculate the vertical divergence between lines caused by vertical GPS drift. Automated Z calibration was the final step employed for relative accuracy calibration.

LiDAR accuracy error sources and solutions:

Type of Error	Source	Post Processing Solution
GPS (Static/Kinematic)	Long Base Lines	None
	Poor Satellite Constellation	None
	Poor Antenna Visibility	Reduce Visibility Mask
Relative Accuracy	Poor System Calibration	Recalibrate IMU and sensor offsets/settings
	Inaccurate System	None
Laser Noise	Poor Laser Timing	None
	Poor Laser Reception	None
	Poor Laser Power	None
	Irregular Laser Shape	None

Operational measures taken to improve relative accuracy:

Low Flight Altitude: Terrain following was employed to maintain a constant above ground level (AGL). Laser horizontal errors are a function of flight altitude above ground (about 1/3000th AGL flight altitude).

Focus Laser Power at narrow beam footprint: A laser return must be received by the system above a power threshold to accurately record a measurement. The strength of the laser return (i.e., intensity) is a function of laser emission power, laser footprint, flight altitude and the reflectivity of the target. While surface reflectivity cannot be controlled, laser power can be increased and low flight altitudes can be maintained.

Reduced Scan Angle: Edge-of-scan data can become inaccurate. The scan angle was reduced to a maximum of $\pm 15^\circ$ from nadir, creating a narrow swath width and greatly reducing laser shadows from trees and buildings.

Quality GPS: Flights took place during optimal GPS conditions (e.g., 6 or more satellites and PDOP [Position Dilution of Precision] less than 3.0). Before each flight, the PDOP was determined for the survey day. During all flight times, a dual frequency DGPS base station recording at 1 second epochs was utilized and a maximum baseline length between the aircraft and the control points was less than 13 nm at all times.

Ground Survey: Ground survey point accuracy (<1.5 cm RMSE) occurs during optimal PDOP ranges and targets a minimal baseline distance of 4 miles between GPS rover and base. Robust statistics are, in part, a function of sample size (n) and distribution. Ground survey points are distributed to the extent possible throughout multiple flightlines and across the survey area.

50% Side-Lap (100% Overlap): Overlapping areas are optimized for relative accuracy testing. Laser shadowing is minimized to help increase target acquisition from multiple scan angles. Ideally, with a 50% side-lap, the nadir portion of one flightline coincides with the swath edge portion of overlapping flightlines. A minimum of 50% side-lap with terrain-followed acquisition prevents data gaps.

Opposing Flightlines: All overlapping flightlines have opposing directions. Pitch, roll and heading errors are amplified by a factor of two relative to the adjacent flightline(s), making misalignments easier to detect and resolve.